Enhancing the sensing specificity of a MoS2 nanosheet-based FRET aptasensor using a surface blocking strategy

Geldert, Alisha; Kenry; Zhang, Xiao; Zhang, Hua; Lim, Chwee Teck

2017

Geldert, A., Kenry, Zhang, X., Zhang, H., & Lim, C. T. (2017). Enhancing the sensing specificity of a MoS2 nanosheet-based FRET aptasensor using a surface blocking strategy. Analyst, 142(14), 2570-2577.

https://hdl.handle.net/10356/86263

https://doi.org/10.1039/C7AN00640C

Enhancing the Sensing Specificity of a MoS_2 Nanosheet-Based FRET Aptasensor

Alisha Geldert[1,#], Kenry[1,2,3,#], Xiao Zhang[5], Hua Zhang[5], Chwee Teck Lim[1,2,3,4,*]

[1]Department of Biomedical Engineering, National University of Singapore, Singapore 117576

[2]NUS Graduate School for Integrative Sciences and Engineering, National University of Singapore, Singapore 117456

[3]Centre for Advanced 2D Materials and Graphene Research Centre, National University of Singapore, Singapore 117543

[4]Mechanobiology Institute, National University of Singapore, Singapore 117411

[5]Center for Programmable Materials, School of Materials Science and Engineering, Nanyang Technological University, Singapore 639798

[#]These authors contributed equally to the work.

*Correspondence

Chwee Teck Lim (ctlim@nus.edu.sg)

Department of Biomedical Engineering

National University of Singapore

9 Engineering Drive 1

Singapore 117576, Singapore

KEYWORDS: Aptamer; pLDH; Transition metal dichalcogenide; MoS_2; FRET.

Abstract

Aptamer-based biosensing, which uses short, single-stranded nucleic acid segments to bind to a target, can be advantageous over antibody-based diagnostics due to the ease of synthesis and high stability of aptamers. However, the development of most aptamer-based sensors (aptasensors) is still in its initial stages and many factors affecting their performance have not been studied in great detail. Here, we develop a MoS_2 nanosheet-based aptasensor using fluorescence resonance energy transfer (FRET) for the detection of the malarial biomarker *Plasmodium* lactate dehydrogenase (pLDH). Based on this scheme, the presence of target is signaled by an increase in fluorescence when fluorescently-labeled aptamers bind to pLDH and release from a quenching material. Interestingly, unlike most of the reported literature on aptasensors, we observe that non-target proteins also cause a considerable increase in the detected fluorescence, which may be due to the nonspecific adsorption of proteins onto the fluorescence quencher leading to the displacement of aptamers from the quencher surface. To reduce this nonspecific association and to enhance the sensor specificity, we propose the application of surface blocking of the quenching material. Importantly, we demonstrate that through surface passivation, the specificity of the MoS_2 nanosheet-based aptasensor towards target pLDH biomolecules can be significantly enhanced, thus contributing to the development of a highly selective and robust point-of-care malaria diagnostics.

Introduction

Point-of-care medical testing benefits greatly from simple biosensors which can accurately and specifically detect and signal the presence of disease biomarkers to enable rapid and accessible disease diagnosis. Conventionally, most rapid diagnostic tests rely on antibodies to bind to biomarkers in a clinical sample. However, aptamers – short, single-stranded nucleic acid segments which can be developed to bind specifically to a range of biomolecules – have gained growing interest as an alternative tool for biosensing in recent years. Aptamers can be selected for essentially any biomolecule through a process known as systematic evolution of ligands by exponential enrichment (SELEX), and many reported aptamers have similar affinity to their targets as antibodies do [1]. As compared to antibody production, aptamer synthesis is affordable and more highly reproducible. Aptamers are also more easily modified with functionalities such as fluorescent labels or biotin tags. They tend to be smaller in size than antibodies, enabling aptamers to be more densely packed on the surface of a sensor for improved sensitivity. Importantly, the nucleic acid composition of aptamers makes them more resistant to

degradation than antibodies, especially in high temperatures and other harsh conditions. Thus, aptamers are potentially cheaper, simpler, and more robust affinity reagents for biosensing applications [2,3].

One simple scheme commonly employed in aptamer-based biosensing (i.e., aptasensing) is fluorescence resonance energy transfer (FRET). In FRET, fluorescently-labeled aptamers are typically combined with a fluorescence quenching material, to which the aptamer will spontaneously adsorb and its fluorescence will be quenched. Upon the addition of an analyte containing the aptamer target, the aptamer will change its conformation to bind to its target, causing the aptamer to be released from the quencher and resulting in a measurable fluorescence increase. In recent years, two-dimensional (2D) nanomaterials, such as graphene-based nanomaterials and transition metal dichalcogenides which have been actively explored for numerous bioapplications [4–8], are increasingly being used as fluorescence quenchers owing to their large specific surface area, high hydrophilicity, and exceptional fluorescence quenching abilities [9,10].

In general, FRET aptasensors are simple and attractive as they operate based on spontaneous adsorption and desorption without the need for complex synthesis or assay procedures. However, the simplicity of FRET-based aptasensors may also limit their sensing performance. In fact, fluorescence quenchers such as graphene oxide (GO), molybdenum disulfide (MoS_2), and other 2D nanomaterials have been found to possess a moderate affinity not only to aptamers but also to a range of proteins [11–13]. Importantly, the nonspecific adsorption of both target and non-target biomolecules onto these fluorescence quenchers may harm sensor performance. The adsorption of target protein molecules onto the surface of quencher reduces the specific signal by reducing the number of target molecules available to bind to and release the aptamers from the quencher surface to recover fluorescence, as was reported with a GO-based aptasensor for ochratoxin A [14]. Furthermore, non-target proteins found in the analyte may also adsorb to the quencher surface and interfere with fluorescence recovery or cause nonspecific recovery, eventually reducing the sensor specificity. Also, the nonspecific adsorption on the quencher surface may raise difficulty in determining the aptamer-to-quencher ratio which maximizes the signal-to-noise ratio. Currently, there has been little investigation into the details involved in FRET-based aptasensing or various factors affecting sensor performance.

Here, we study the use of aptamers for the detection of a malarial biomarker, *Plasmodium* lactate dehydrogenase (pLDH). The aptamer-based detection of pLDH is highly attractive as the current antibody-based pLDH-targeted rapid diagnostic tests suffer from poor performance in hot and humid conditions in which malaria is prevalent, such as in tropical climates [15,16]. We first investigate the interactions between pLDH aptamer and its target as well as nonspecific proteins typically found in a blood sample. This aptamer is then incorporated into a FRET-based aptasensor and the specificity of the aptasensor is characterized. We show that the aptasensor is capable of detecting pLDH, although common plasma proteins also induce unexpectedly high levels of nonspecific fluorescence recovery. In light of our experimental data, we propose that this nonspecific recovery may be caused by proteins adsorbing nonspecifically onto the fluorescence quencher and displacing aptamers from its surface. To mitigate this nonspecific protein adsorption, the quencher surface is blocked in order to improve the sensor specificity significantly. Although literatures have reported the coating of quenching materials in a FRET-based aptasensing scheme with blocking agents, the underlying motivation as well as the effect of this blocking have not been clearly demonstrated [14,17,18]. As such, through this work, we aim to investigate the mechanism of nonspecific fluorescence recovery in FRET-based aptasensors and demonstrate the application of surface blocking in enhancing their sensing specificity.

Results and Discussion

An aptamer which has been demonstrated to bind to pLDH [19], with the fluorescent dye FAM conjugated to the 3' end, was employed throughout this study. We first characterized the optical properties of the aptamer using absorbance, fluorescence, and circular dichroism (CD) spectroscopy. The aptamer possessed an absorbance peak at around 505 nm and a fluorescence peak at around 525 nm (**Fig. 1a**), which is characteristic of the FAM dye. This showed that the free aptamer can produce a detectable fluorescent signal, which is crucial to FRET-based sensing. Proper aptamer folding is also required to form the specific stem, loop, or quadruplex structures necessary for target recognition and binding. Because aptamer folding is dependent on temperature, ionic concentration of the solvent, and many other factors [20,21], we aimed to ensure that the pLDH aptamer could fold into its proper conformation in the prepared buffer solution, even with its fluorescent label. To do this, the CD spectrum of the aptamer was characterized and we observed that the spectrum exhibited a characteristic positive peak near 280 nm and negative peak near 240 nm (**Fig. 1b**), matching closely with that reported in literature. Altogether, these results suggested that the pLDH aptamer used here had proper

fluorescence and secondary structure to bind to its target and produce a detectable signal corresponding to the presence of target biomolecule.

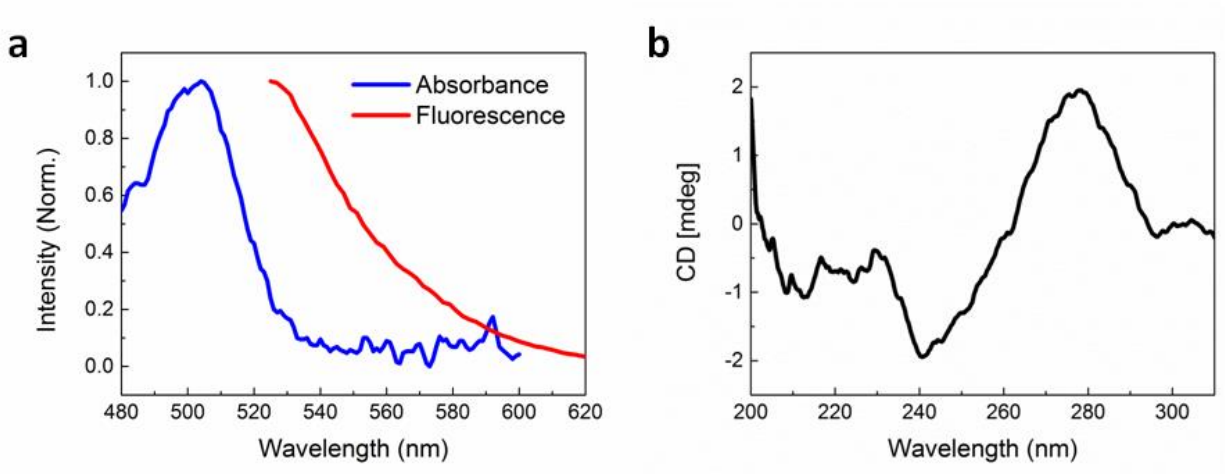

Figure 1 | Characterization of the fluorescently-labeled pLDH aptamer. (a) Normalized absorbance and fluorescence of the pLDH aptamer. Fluorescence measurements were taken at an excitation wavelength of 495 nm, corresponding to the absorbance maximum of the FAM dye label. (b) CD spectrum of the pLDH aptamer, with negative and positive peaks around 240 nm and 280 nm, respectively.

In order to have a diagnostic value, the aptamer must bind specifically to the target pLDH and not to other biomolecules so as to minimize false positive test results. As such, we used CD spectroscopy to probe the interactions between pLDH aptamer and both pLDH protein (**Fig. 2a**) and common plasma proteins (i.e., fibrinogen (**Fig. 2b**), globulin (**Fig. 2c**), and albumin (**Fig. 2d**)) present in a blood sample. The CD spectra of aptamer-protein mixtures were measured at several timepoints: immediately and after 30 and 60 minutes of incubation. In the far-UV range (i.e., < 250 nm), the protein CD spectra exhibited negative peaks associated with the alpha helix and beta sheet secondary structures, while the aptamer CD spectrum remained near zero. Thus, differences in the 200-250 nm range of the CD spectra of aptamer-protein mixtures may be attributed to changes in protein structure as the aptamer contributes negligibly to the CD spectrum at this wavelength range. Similarly, at around 280 nm, the CD spectrum of the pLDH aptamer displayed a peak (albeit smaller due to the lesser chirality of single-stranded DNA), while the CD spectra of all tested proteins were near zero. Thus, changes in the 280 nm peak in the CD spectra of aptamer-protein mixtures represent changes in the aptamer structure.

Aptamer-ligand binding is typically described by an induced-fit model, in which a ligand induces an aptamer to fold to precisely fit the ligand. As such, the aptamer undergoes a more significant conformational change than its target when the two bind [22]. According to this model, we would anticipate the CD peak corresponding to the aptamer to be altered when the aptamer is incubated with its target, reflecting the change in aptamer structure induced by its target ligand. Previous studies have reported changes in the aptamer peak of the CD spectrum when aptamers bound to targets such as L-tyrosinamide [23] and thrombin [24]. Similarly, we observed a distinct change in the shape of the aptamer peak at 280 nm when pLDH aptamer was incubated with its target, pLDH protein (**Fig. 2a**). As the aptamer and its target were incubated for longer durations, the signal intensity near 280 nm decreased, forming a spectrum with two smaller peaks on either side of 280 nm. When the aptamer was incubated with nonspecific proteins, however, the 280 nm peak retained its original shape (**Fig. 2b** to **Fig. 2d**). This indicated that the structure of the pLDH aptamer changed more significantly when it was incubated with pLDH protein than with nonspecific proteins, which suggested that the aptamer bound specifically to its target.

In contrast, when pLDH aptamer was incubated with its target, pLDH protein, the magnitude and shape of the negative peak of the CD spectra remained relatively constant over time. This suggested that the aptamer did not significantly alter the structure of the target protein upon binding, which is important to alternative sensing schemes taking advantage of the enzymatic function of pLDH and requiring the protein to maintain its structure and function. For instance, a recently-reported biosensor coupled the pLDH-catalyzed conversion of lactate to pyruvate with a colorimetric reaction to indicate the presence of pLDH [25]. Surprisingly, as the pLDH aptamer was incubated with nonspecific plasma proteins for increasing amounts of time, the magnitude and shape of the negative peak varied considerably. This indicated that the pLDH aptamer interacted with nonspecific proteins and induced changes to the protein structures, though this does not necessarily indicate aptamer-protein binding.

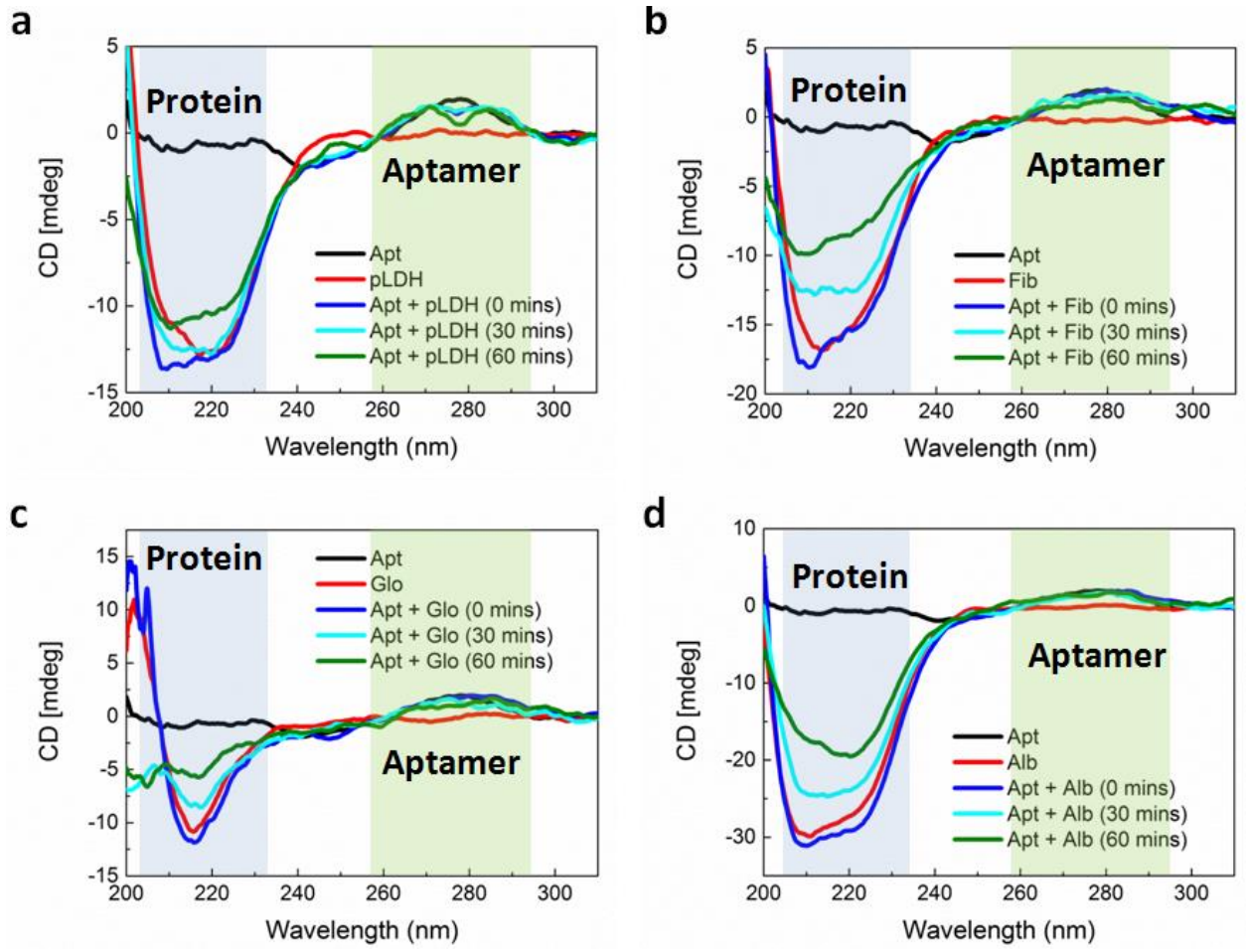

Figure 2 | CD spectra of aptamer, proteins, and aptamer-protein mixtures. The CD spectra of 5 µM pLDH aptamer (Apt), 2.5 µM of: (a) pLDH, (b) fibrinogen (Fib), (c) globulin (Glo), and (d) albumin (Alb) proteins, and 5 µM pLDH aptamer incubated with 2.5 µM proteins for varying durations.

To further assess the specificity of the aptamer, we performed a binding assay in which fluorescently-labeled pLDH aptamer was incubated on top of a protein-coated surface for 10 minutes and then rinsed to wash away any unbound aptamer. Areas which fluoresced after the rinsing process indicated the occurrence of aptamer-protein binding. Here, we observed more fluorescent regions on the pLDH-coated surface (**Fig. 3a**) as compared to the fibrinogen-, globulin-, and albumin-coated surfaces (**Fig. 3b to Fig. 3d**), supporting our earlier finding that pLDH aptamer binds specifically to its target. The results were further quantified by measuring the fluorescent area in images from several random locations on each protein surface (**Fig. 3e**). Though the fluorescent area observed in the aptamer-pLDH incubation varied between images, the specific pairing exhibited a much higher total amount of aptamer-protein binding than any of the nonspecific incubations, which all had a negligible total fluorescent area.

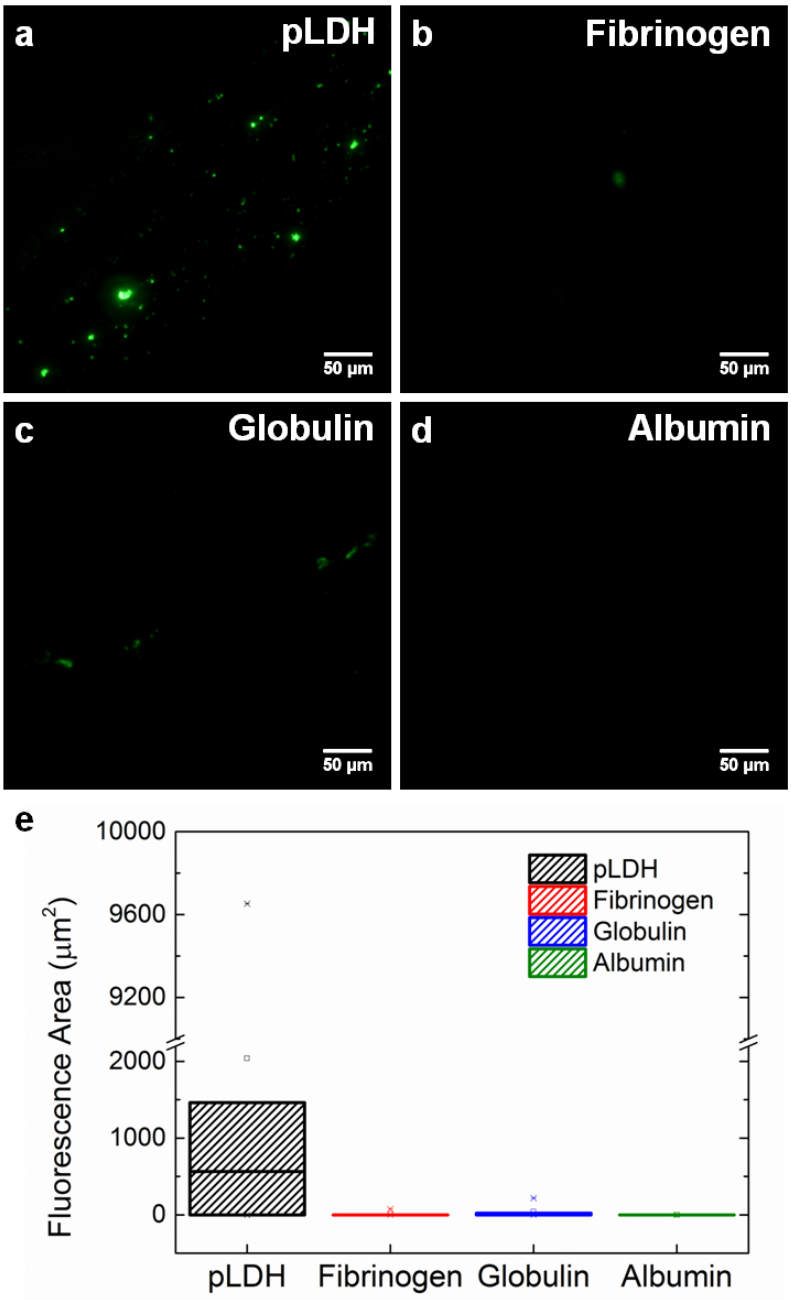

Figure 3 | Aptamer-protein binding assay. Fluorescent areas indicate the binding between pLDH aptamer and (a) pLDH, (b) fibrinogen, (c) globulin, or (d) albumin protein. 7.16 µM of protein was adsorbed onto a mica surface, on top of which 10 µM fluorescently-labeled pLDH aptamer was incubated and then rinsed. (e) Box plot quantifying the fluorescent areas measured from images at six randomly chosen locations for each aptamer-protein incubation. The higher number of fluorescent areas observed in the pLDH aptamer-pLDH protein incubation shows that pLDH aptamer binds specifically to its target.

After investigating the aptamer-protein interactions and verifying the proper functionality of pLDH aptamer, we incorporated the aptamer into a FRET sensing assay. Fluorescently-labeled pLDH aptamer was incubated with MoS_2 nanosheets which had been synthesized and characterized in our previous work, for 10 minutes to allow the aptamer to adsorb to and be quenched by the nanosheets. Subsequently, an analyte solution containing pLDH or a nonspecific protein was added to the aptamer-MoS_2 incubation, and fluorescence readings were taken after 30 minutes to measure the amount of recovery induced by the protein. Although our previous experimental results on the interactions between pLDH aptamer and a wide range of proteins suggested that pLDH binds specifically to its target, intriguingly, the plasma proteins fibrinogen, globulin, and albumin all induced considerable fluorescence recovery of almost half the magnitude of that of the specific recovery due to pLDH (**Fig. 4a,** Unblocked bars).

As our characterization data (**Fig. 2** and **Fig. 3**) indicate that the aptamer binds specifically to pLDH, we hypothesized that the observed nonspecific fluorescence recovery was not primarily caused by nonspecific proteins binding to the aptamer and releasing it from the MoS_2 nanosheet surface. Instead, it is possible that the nonspecific proteins adsorbed to the MoS_2 nanosheet and displaced the aptamers from the nanosheet surface, causing the aptamer fluorescence to be restored. In this case, preventing nonspecific protein adsorption onto the nanosheet surface should reduce the amount of nonspecific fluorescence recovery (**Scheme 1**). In fact, nonspecific protein adsorption has been known to pose challenges to the development of various biomedical applications, notably biomedical implants. One common strategy to combat nonspecific protein adsorption on implants is to immobilize blocking molecules on the surface of the biomaterial, as Kenausis et al. demonstrated by coating metal oxide surfaces with a blocking agent to reduce the adsorption of fibrinogen, albumin, and other serum proteins [26]. Motivated by this, we implemented a similar blocking strategy, using bovine serum albumin (BSA) as a blocking agent to coat the nanosheet surface and prevent nonspecific protein adsorption. BSA, in general, possesses surface passivation effect and has been actively utilized as an inexpensive surface blocking agent to mitigate nonspecific adsorption on photoresists, polystyrene, and other materials [27–29]. However, BSA has rarely been explored as a blocking agent for 2D nanomaterials.

For blocked samples, BSA was incubated with the aptamer-nanosheet solution for 10 minutes prior to analyte addition to allow it to adsorb to available spaces on the nanosheet surface. The fluorescence recovery due to BSA alone was subtracted from fluorescence recovery of blocked

samples after analyte addition to account for any aptamer displacement caused by BSA. Interestingly, we observed that although the recovery due to pLDH was slightly lower in the blocked case, the recovery due to nonspecific proteins decreased to a large extent when blocking was applied (**Fig. 4a**). In fact, the ratio of the fluorescence recovery induced by pLDH to the recovery induced by nonspecific proteins, which was used as a signal-to-noise metric, was significantly higher when BSA blocking was implemented as compared to when the analyte was added directly to the unblocked aptamer-MoS_2 nanosheet incubation (**Fig. 4b**). Particularly, the pLDH fluorescence recovery was only about twice as high as nonspecific protein recovery in unblocked samples, while in blocked samples, the specific pLDH fluorescence recovery was at least four times as high as the nonspecific recovery. Also, the effect of BSA blocking was not concentration-dependent as a wide range of BSA concentrations generated similar signal-to-noise ratios. Ultimately, in all cases, BSA blocking resulted in higher ratios of pLDH-induced to nonspecific protein-induced fluorescence recovery, demonstrating that surface blocking of the fluorescence quencher can reduce the background signal. As it requires only one additional incubation step, blocking serves as an attractive strategy to significantly improve sensor specificity while maintaining the simplicity of the FRET-based aptasensing technique.

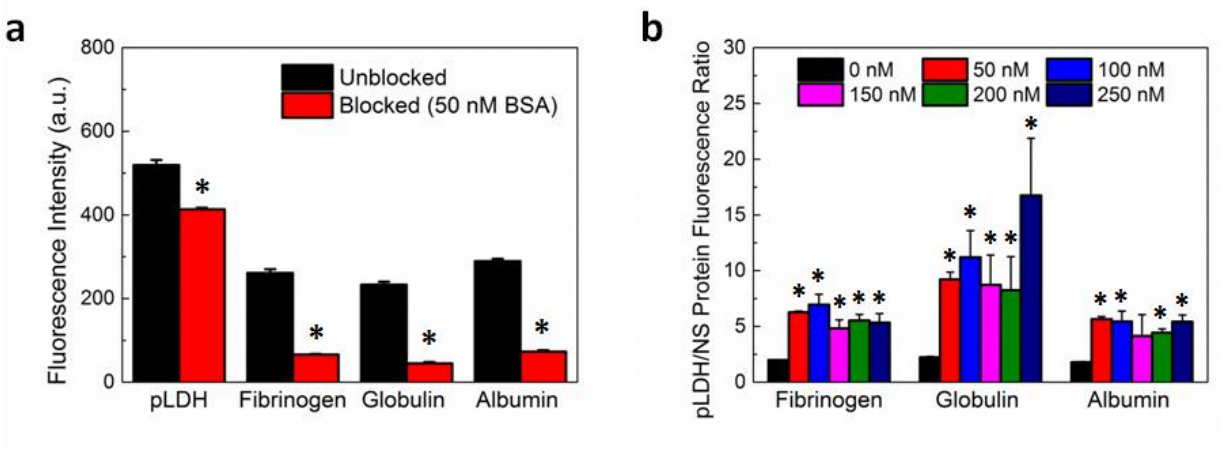

Figure 4 | Effect of surface blocking on the sensing specificity of the pLDH aptasensor. (a) Fluorescence intensity after the addition of 250 nM protein to either an aptasensor which was unblocked or blocked with 50 nM BSA. (b) Ratio of the fluorescence measured after the addition of 250 nM pLDH protein to the fluorescence measured after the addition of 250 nM of a nonspecific protein when the aptasensor was blocked with varying concentrations of BSA. All fluorescence measurements were taken with an excitation wavelength of 495 nm and an emission wavelength of 527 nm. The * indicates that the fluorescence ratio is significantly different than that of the unblocked sample (i.e., $p < 0.05$).

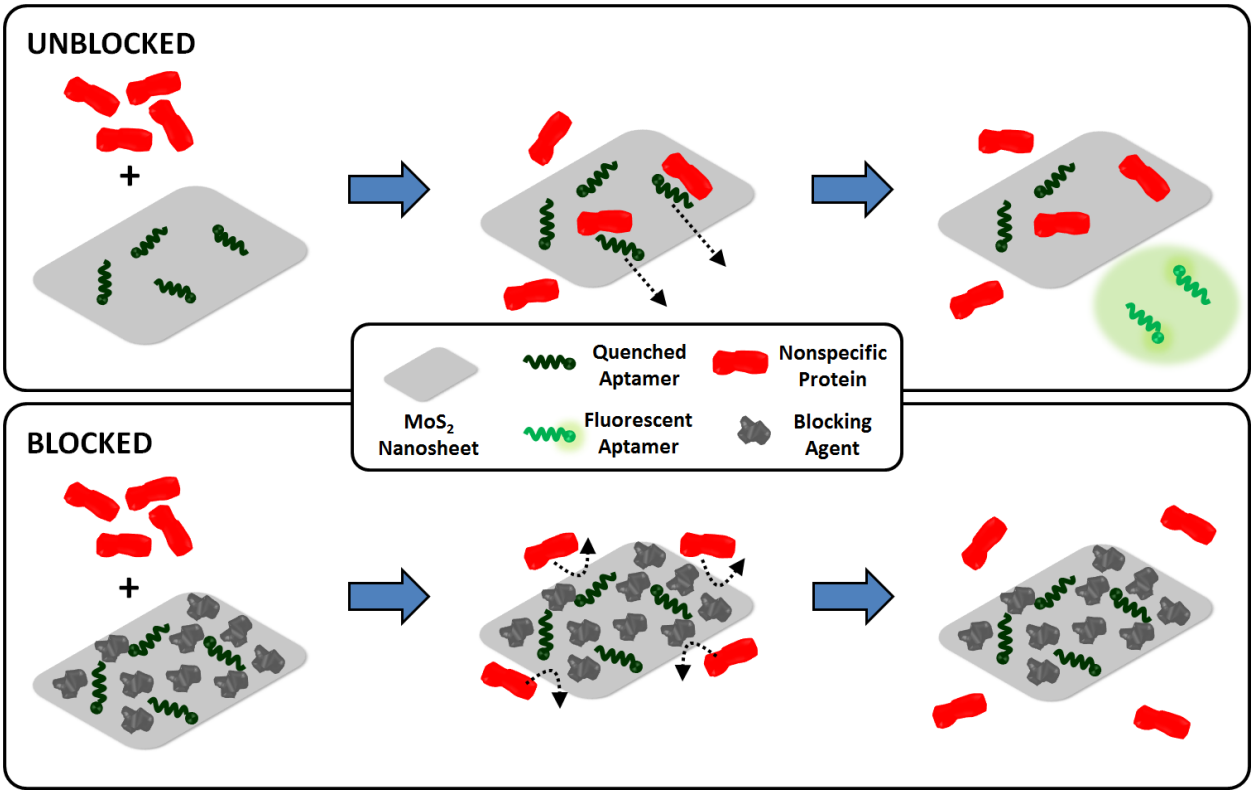

Scheme 1 | Effect of MoS_2 nanosheet surface blocking on nonspecific fluorescence recovery. We hypothesize that when the nanosheet is unblocked, nonspecific proteins may adsorb onto the nanosheet surface and aptamers may be displaced from the surface, restoring the aptamers' fluorescence. By blocking the surface of the nanosheet, the amount of available space on the nanosheet will be reduced. This will prevent the adsorption of nonspecific proteins onto the nanosheet and the aptamer displacement from the quencher surface, reducing the amount of nonspecific fluorescence recovery significantly.

Conclusions

We investigated the interactions of an aptamer for a malarial biomarker, pLDH, with both its target and with nonspecific plasma proteins commonly present in a blood sample and developed a MoS_2 nanosheet-based FRET aptasensor for the diagnosis of malaria. To improve the specificity of the sensor, we adopted a blocking strategy in which the surface of the fluorescence quenching nanosheets was passivated with BSA prior to analyte addition. This significantly reduced the fluorescence recovery induced by nonspecific proteins, most likely by preventing them from binding to the quencher and displacing the aptamers from the quencher surface. Interestingly, this simple sensor requires only the mixing of aptamer, quencher, blocking agent, and protein solutions, and the entire test can be completed rapidly. We believe that this study has provided useful insight into various factors affecting FRET-based aptasensor

performance and demonstrated the successful combination of this technique with a blocking strategy to detect the malarial biomarker pLDH with high specificity against other proteins commonly found in the blood, supporting the development of a simple and stable rapid diagnostic test for malaria.

Methods

Materials

MoS_2 nanosheets were synthesized using the previously-reported electrochemical lithium intercalation method [10,30]. Fluorescently-labeled pLDH aptamer with the sequence 5'- GTT CGA TTG GAT TGT GCC GGA AGT GCT GGC TCG AAC - FAM - 3' was ordered from Integrated DNA Technologies. The aptamer was dissolved in a buffer of 20 mM Tris-HCl, 50 mM NaCl, 5 mM KCl, and 5 mM $MgCl_2$ (pH 8). Recombinant *falciparum* pLDH protein was purchased from Sino Biological and dissolved in water, as per the manufacturer's instructions. All other proteins were purchased from Sigma Aldrich and dissolved in 1× PBS.

Circular Dichroism

CD spectra were measured with a Jasco J-810 spectropolarimeter with a scan speed of 500 nm/min, using a cuvette with a 0.1 cm path length. All reported spectra are an average of five scans. The final concentrations of aptamer and protein were 5 µM and 2.5 µM, respectively, for all measurements.

Microscopy Binding Assay

7.16 µM of either pLDH or a nonspecific protein was incubated on top of freshly cleaved mica for 10 minutes to allow the protein to adsorb to the surface. Subsequently, 10 µM of fluorescently-labeled pLDH aptamer was incubated on top of the protein-coated surface for 10 minutes. The mica surface was then rinsed three times with water and left to dry for 5 minutes. Images of six randomly-chosen regions on the mica were taken with a fluorescence microscope. All images were taken at 20× with 1 second exposure.

Image Processing

To quantify the fluorescent area in each set of images, all images were background-subtracted and converted to 8-bit. A threshold range of 18-255 was applied to distinguish between fluorescent and non-fluorescent areas. Total fluorescent areas were measured using the

Analyze Particles function in ImageJ. All fluorescent areas larger than 0.025 um^2 were considered.

Absorbance and Fluorescence Measurements

All absorbance measurements were taken with a Nanodrop 2000 UV-vis spectrophotometer, and all fluorescence measurements were taken with a Tecan Infinite M200 microplate reader. The reported absorbance and fluorescence spectra of the aptamer are an average of three independent readings and were normalized using the formula

$$\frac{I - I_{min}}{I_{max} - I_{min}} \quad (1)$$

where I is the absorbance or fluorescence intensity of the sample.

For fluorescence recovery experiments, 100 nM pLDH aptamer was incubated with 20 µg/mL MoS_2 for 10 minutes to allow for the aptamer to adsorb to and be quenched by the MoS_2 surface. For unblocked samples, 250 nM of either pLDH or a nonspecific protein was then added to the aptamer-MoS_2 solution. For blocked samples, BSA (at 50-250 nM, depending on the experiment) was added to the aptamer-MoS_2 solution and incubated for an additional 10 minutes prior to 250 nM protein addition. In one blocked sample, PBS was added instead of protein, to assess the amount of fluorescence recovery caused solely by the blocking agent. The fluorescence of this sample (block + PBS) was subtracted from the fluorescence of other blocked samples (block + 250 nM protein) to account for the additional recovery caused by the blocking agent itself. All concentrations are reported as the final concentrations in each sample, and all samples had a total volume of 200 µL. Fluorescence intensity was measured 30 minutes after protein (or PBS) was added to the solution. Each reported value is the average of measurements from three independent samples.

Acknowledgements

This research was supported by the National Research Foundation, Prime Minister's Office, Singapore under its medium-sized centre programme, Centre for Advanced 2D Materials and its Research Centre of Excellence, Mechanobiology Institute, as well as the

MechanoBioEngineering Laboratory of the Department of Biomedical Engineering of the National University of Singapore.

This work was also supported by MOE under AcRF Tier 2 (ARC 26/13, No. MOE2013-T2-1-034; ARC 19/15, No. MOE2014-T2-2-093; MOE2015-T2-2-057) and AcRF Tier 1 (RG5/13), NTU under Start-Up Grant (M4081296.070.500000) and iFood Research Grant (M4081458.070.500000), and Singapore Millennium Foundation. Kenry and A. Geldert would like to acknowledge the NUS Graduate School for Integrative Sciences and Engineering Scholarship and Whitaker International Program Fellowship, respectively.

References

1. Jayasena, S. D. Aptamers: An Emerging Class of Molecules That Rival Antibodies in Diagnostics. *Clin. Chem.* **45,** 1628–1650 (1999).
2. Groff, K., Brown, J. & Clippinger, A. J. Modern affinity reagents: Recombinant antibodies and aptamers. *Biotechnol. Adv.* **33,** 1787–1798 (2015).
3. Zhou, W., Huang, P.-J. J., Ding, J. & Liu, J. Aptamer-based biosensors for biomedical diagnostics. *Analyst* **139,** 2627–2640 (2014).
4. Kenry, Loh, K. P. & Lim, C. T. Molecular Hemocompatibility of Graphene Oxide and Its Implication for Antithrombotic Applications. *Small* **11,** 5105–5117 (2015).
5. Kenry *et al.* Highly Flexible Graphene Oxide Nanosuspension Liquid-Based Microfluidic Tactile Sensor. *Small* **12,** 1593–1604 (2016).
6. Kenry, Chaudhuri, P. K., Loh, K. P. & Lim, C. T. Selective Accelerated Proliferation of Malignant Breast Cancer Cells on Planar Graphene Oxide Films. *ACS Nano* **10,** 3424–3434 (2016).
7. Lee, W. C. *et al.* Cell-Assembled Graphene Biocomposite for Enhanced Chondrogenic Differentiation. *Small* **11,** 963–969 (2015).
8. Ng, A. M. H., Kenry, Teck Lim, C., Low, H. Y. & Loh, K. P. Highly sensitive reduced graphene oxide microelectrode array sensor. *Biosens. Bioelectron.* **65,** 265–273 (2015).
9. Lu, C.-H., Yang, H.-H., Zhu, C.-L., Chen, X. & Chen, G.-N. A Graphene Platform for Sensing Biomolecules. *Angew. Chem. Int. Ed.* **48,** 4785–4787 (2009).
10. Zhu, C. *et al.* Single-Layer MoS2-Based Nanoprobes for Homogeneous Detection of Biomolecules. *J. Am. Chem. Soc.* **135,** 5998–6001 (2013).
11. Lee, J. *et al.* Two-dimensional Layered MoS2 Biosensors Enable Highly Sensitive Detection of Biomolecules. *Sci. Rep.* **4,** 7352 (2014).
12. Zhang, J. *et al.* Graphene Oxide as a Matrix for Enzyme Immobilization. *Langmuir* **26,** 6083–6085 (2010).

13. Zuo, G., Zhou, X., Huang, Q., Fang, H. & Zhou, R. Adsorption of Villin Headpiece onto Graphene, Carbon Nanotube, and C60: Effect of Contacting Surface Curvatures on Binding Affinity. *J. Phys. Chem. C* **115,** 23323–23328 (2011).
14. Sheng, L., Ren, J., Miao, Y., Wang, J. & Wang, E. PVP-coated graphene oxide for selective determination of ochratoxin A via quenching fluorescence of free aptamer. *Biosens. Bioelectron.* **26,** 3494–3499 (2011).
15. McMorrow, M. L., Aidoo, M. & Kachur, S. P. Malaria rapid diagnostic tests in elimination settings—can they find the last parasite? *Clin. Microbiol. Infect. Off. Publ. Eur. Soc. Clin. Microbiol. Infect. Dis.* **17,** 1624–1631 (2011).
16. Wongsrichanalai, C., Barcus, M. J., Muth, S., Sutamihardja, A. & Wernsdorfer, W. H. A Review of Malaria Diagnostic Tools: Microscopy and Rapid Diagnostic Test (RDT). *Am. J. Trop. Med. Hyg.* **77,** 119–127 (2007).
17. Peng, L., Zhu, Z., Chen, Y., Han, D. & Tan, W. An exonuclease III and graphene oxide-aided assay for DNA detection. *Biosens. Bioelectron.* **35,** 475–478 (2012).
18. Pu, Y. *et al.* Insulin-binding aptamer-conjugated graphene oxide for insulin detection. *Analyst* **136,** 4138–4140 (2011).
19. Lee, S. *et al.* A highly sensitive aptasensor towards Plasmodium lactate dehydrogenase for the diagnosis of malaria. *Biosens. Bioelectron.* **35,** 291–296 (2012).
20. Baldrich, E., Restrepo, A. & O'Sullivan, C. K. Aptasensor Development: Elucidation of Critical Parameters for Optimal Aptamer Performance. *Anal. Chem.* **76,** 7053–7063 (2004).
21. Kankia, B. I. & Marky, L. A. Folding of the Thrombin Aptamer into a G-Quadruplex with Sr2+: Stability, Heat, and Hydration. *J. Am. Chem. Soc.* **123,** 10799–10804 (2001).
22. Hermann, T. & Patel, D. J. Adaptive Recognition by Nucleic Acid Aptamers. *Science* **287,** 820–825 (2000).
23. Lin, P.-H. *et al.* Microcalorimetrics Studies of the Thermodynamics and Binding Mechanism between l-Tyrosinamide and Aptamer. *J. Phys. Chem. B* **112,** 6665–6673 (2008).
24. Lin, P.-H. *et al.* Studies of the binding mechanism between aptamers and thrombin by circular dichroism, surface plasmon resonance and isothermal titration calorimetry. *Colloids Surf. B Biointerfaces* **88,** 552–558 (2011).
25. Dirkzwager, R. M., Kinghorn, A. B., Richards, J. S. & Tanner, J. A. APTEC: aptamer-tethered enzyme capture as a novel rapid diagnostic test for malaria. *Chem. Commun.* **51,** 4697–4700 (2015).
26. Kenausis, G. L. *et al.* Poly(l-lysine)-g-Poly(ethylene glycol) Layers on Metal Oxide Surfaces: Attachment Mechanism and Effects of Polymer Architecture on Resistance to Protein Adsorption. *J. Phys. Chem. B* **104,** 3298–3309 (2000).
27. Convert, L. *et al.* Passivation of KMPR microfluidic channels with bovine serum albumin (BSA) for improved hemocompatibility characterized with metal-clad waveguides. *Sens. Actuators B Chem.* **173,** 447–454 (2012).

28. Jeyachandran, Y. L., Mielczarski, J. A., Mielczarski, E. & Rai, B. Efficiency of blocking of non-specific interaction of different proteins by BSA adsorbed on hydrophobic and hydrophilic surfaces. *J. Colloid Interface Sci.* **341,** 136–142 (2010).
29. Reimhult, K., Petersson, K. & Krozer, A. QCM-D analysis of the performance of blocking agents on gold and polystyrene surfaces. *Langmuir ACS J. Surf. Colloids* **24,** 8695–8700 (2008).
30. Zeng, Z. *et al.* Single-Layer Semiconducting Nanosheets: High-Yield Preparation and Device Fabrication. *Angew. Chem. Int. Ed.* **50,** 11093–11097 (2011).